

Zeitschrift: IABSE reports = Rapports AIPC = IVBH Berichte
Band: 37 (1982)

Artikel: Fatigue strength of reinforced concrete slabs under moving loads
Autor: Sonoda, K. / Horikawa, T.
DOI: <https://doi.org/10.5169/seals-28942>

Nutzungsbedingungen

Die ETH-Bibliothek ist die Anbieterin der digitalisierten Zeitschriften auf E-Periodica. Sie besitzt keine Urheberrechte an den Zeitschriften und ist nicht verantwortlich für deren Inhalte. Die Rechte liegen in der Regel bei den Herausgebern beziehungsweise den externen Rechteinhabern. Das Veröffentlichen von Bildern in Print- und Online-Publikationen sowie auf Social Media-Kanälen oder Webseiten ist nur mit vorheriger Genehmigung der Rechteinhaber erlaubt. [Mehr erfahren](#)

Conditions d'utilisation

L'ETH Library est le fournisseur des revues numérisées. Elle ne détient aucun droit d'auteur sur les revues et n'est pas responsable de leur contenu. En règle générale, les droits sont détenus par les éditeurs ou les détenteurs de droits externes. La reproduction d'images dans des publications imprimées ou en ligne ainsi que sur des canaux de médias sociaux ou des sites web n'est autorisée qu'avec l'accord préalable des détenteurs des droits. [En savoir plus](#)

Terms of use

The ETH Library is the provider of the digitised journals. It does not own any copyrights to the journals and is not responsible for their content. The rights usually lie with the publishers or the external rights holders. Publishing images in print and online publications, as well as on social media channels or websites, is only permitted with the prior consent of the rights holders. [Find out more](#)

Download PDF: 01.04.2026

ETH-Bibliothek Zürich, E-Periodica, <https://www.e-periodica.ch>



Fatigue Strength of Reinforced Concrete Slabs under Moving Loads

Résistance à la fatigue des dalles en béton armé sous des charges mobiles

Ermüdungsfestigkeit von Stahlbetonplatten unter beweglichen Lasten

K. SONODA

Professor
Osaka City University
Osaka, Japan

T. HORIKAWA

Res. Associate
Osaka City University
Osaka, Japan

SUMMARY

Twenty models of a reinforced concrete bridge deck slab were tested under static loading, fixed point pulsating loading and repetitive moving loads. These moving loads were applied along several lines to simulate the passage of truck wheels. Under these loadings, differences in cracking pattern, deflection growth, reinforcement stresses and load carrying capacity are examined.

RESUME

Vingt modèles de dalles en béton armé pour ponts-routes ont été essayés sous charge statique, charge fixe pulsative et charges mobiles répétées. Ces charges mobiles ont été appliquées le long de plusieurs lignes pour simuler le passage de roues de camion. Sous ces charges, des différences dans la fissuration, l'augmentation des flèches, les contraintes des aciers et la capacité portante ont été examinées.

ZUSAMMENFASSUNG

Insgesamt zwanzig Modelle von Stahlbeton-Fahrbahntafeln wurden unter statischer Last, pulsierender Last mit festem Lastpunkt, sowie unter wiederholter beweglicher Last geprüft. Die beweglichen Lasten sollten die Schwerverkehrslasten wirklichkeitsnah simulieren. Die Unterschiede in den Beanspruchungen wie Risszustand, Zunahme der Durchbiegung, Spannung in der Bewehrung sowie das Tragvermögen wurden untersucht.



1. INTRODUCTION

Since bridge deck slabs directly sustain repeated moving wheel loads, they have more the possibility of fatigue failure than other members of the bridge such as beams and girders. In particular, a reinforced concrete deck slab (RC slab) may undergo the influence of fatigue on both sides of inherent strengths of materials and bond strengths between dissimilar materials. However, there has no design code for bridge deck RC slabs in any country, taking into consideration of fatigue effect directly. The reasons for this seem to stem from the understanding that the ultimate load carrying capacities of RC slabs are very large and a conventional design code based on an allowable stress method is too conservative to require consideration of fatigue effect.

In Japan, since about 1965, however, fatigue damage followed by a peeling off of concrete covering bottom reinforcements or a depression of pavement due to punching failure of slab has often occurred, especially in RC deck slabs supported by steel girders. Considering that the resulting damage is so severe as to interfere with the serviceability of bridge deck after the passage of only several years following the opening for service, we must emphasize that the effect of fatigue must be considered in the stage of design, though other factors such as the recent increase of traffic load intensity and the incompleteness of fabrication should perhaps also be included among the cause.

Recently, some fatigue tests of model or prototype RC deck slabs were carried out under central or eccentric pulsating loading through a hydraulic jack [1,2,3]. But such a loading condition is not sufficient to reveal the fatigue characteristics of bridge deck slabs because cracking patterns under the loadings applied at a fixed point were of a radial form spreading from the loading point which differed substantially from a grid-like or tortoiseshell-like form observed in actually damaged deck slabs, and furthermore, the fatigue failure mode in the tests often followed fracture of reinforcements but the failure modes observed in actually damaged slabs were not associated with any fracture of reinforcements.

The purpose of this paper is to clarify the fatigue characteristics of RC deck slabs under repeated moving wheel loads. A total of 20 model slabs of about 1/3 scale to one panel between adjacent main girders of a typical steel-concrete composite girder bridge were tested under static loading, pulsating loading at a fixed point and repeated moving loadings on several different points used to simulate the travelling of wheel loads. In particular, differences in cracking pattern, growth of deflection, stresses of reinforcements and load carrying capacities under these loading conditions are discussed.

2. DESCRIPTION OF SPECIMENS AND TESTS

The details of test slabs are shown in Table 1. The slabs marked " I " have isotropic bottom reinforcements, while the slabs marked " O " have orthotropic bottom reinforcements whose transverse reinforcements, arranged in parallel to the longer side of the slabs, are reduced to half the amount of the longitudinal ones. The reinforcement-ratio in longitude was 1.32% which corresponded to a moderate amount in RC deck slabs designed by the current Japanese code. The sizes of the test slabs were 90 cm long, 260 cm wide, and 6.0 cm thick. The test slabs were simply supported over two way spans, 80 cm and 250 cm, respectively, and their aspect ratio, about 3.0, was chosen so as to approximately reflect the characteristics of one-way slab supported by adjacent steel girders.

Test programs are shown in Table 2. A single concentrated load was applied

through a rubber pad 1.0 cm thick which was stuck to a steel plate 0.5 cm thick, and the contact area of the rubber pad to the top surface of the slab was taken as 17 cm x 7 cm which corresponded to about 1/3 scale of the contact area of a rear wheel tire of the truck specified by the Japanese code. Four types of loading were used in the tests, static, pulsating at a fixed point, repeated moving on a single track along the transversal center line, A-A, shown in Fig. 1 and repeated moving on three tracks, A-A, B-B, and C-C, in the figure. The moving loadings on a single track were carried out in such a way as to move the concentrated load every one cycle of loading at each discrete point in the transverse direction. While the moving loadings on the three tracks were carried out by changing cyclically a loading track after 100 rounds of moving loadings along each track. Load levels, namely the ratio of a repeated load to a static collapse load, were set approximately at 50, 55, 60, 65, 75, 80 and 85%, where the static collapse loads were determined by the results of the slabs IS and OS apriori tested. The rate of loading ranged from 3 Hz to 4 Hz in the pulsating loading and was about 1 Hz per each point in the moving loadings. A electro-hydraulic loading machine was used and the movement of load was carried out by moving the actuator by hand.

3. MATERIAL PROPERTIES

The concrete used in the test slabs consisted of ordinary portland cement with a unit weight 370 kg/m^3 , water-cement ratio 0.5, aggregate-cement ratio 5.0, and maximum size of crushed gravels 1.5 cm, and the slump of fresh concrete was 12 cm and the average compressive strength in cylinder at the age of 28 days was 28.3 MN/m^2 . The reinforcements consisted of round steel bars of diameter, 6 mm, whose average yield stress and average tensile strength were 255 MN/m^2 and 314 MN/m^2 , respectively. All of the test slabs were cast simultaneously and were cured in air until the time of testing after 40 - 240 days since the casting.

4. OBSERVATIONS AND RESULTS

4.1 Static strength

The slabs IS and OS were tested under a static loading. The design load for the slabs allowable in the Japanese code, namely the load giving an allowable tensile stress, 138 MN/m^2 , in the bottom reinforcements, corresponds to 12.9 kN.

In the isotropic slab IS, initial cracking on the bottom side was observed at the design load mentioned above, while crack on the top side was first observed at the load, 39 kN. In the orthotropic slab OS, initial bottom surface cracking and top surface cracking were noted at the loads, 12.9 kN and 34.3 kN, respectively. The cracking patterns on the bottom surfaces were of a radial form, spreading from the loading point, and the collapse mode was of the

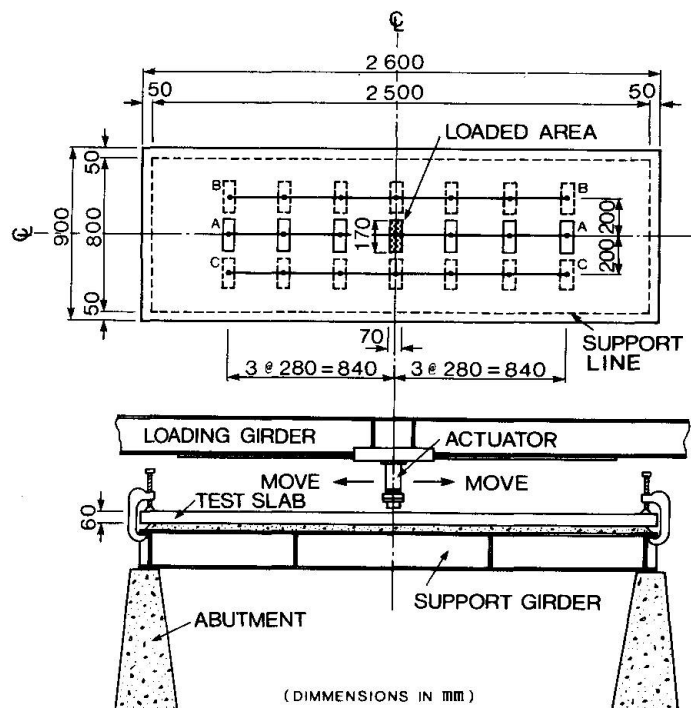


Fig. 1 Test Setup.



punching shear type following a flexural failure mode which had partially proceeded.

Since the collapse modes were located within the vicinity of the loading point, three tests about the center point and other two points of ± 70 cm away from this point on the transversal center line were carried out for each slab. The average value of the collapse loads obtained was 62.3 kN in the slab IS and 58.1 kN in the slab OS, theoretical values of which were 61.7 kN and 55.6 kN, respectively, using the yield line theory, assuming a circular or elliptical fan of yield lines, and considering the hogging plastic moment of cross section having effective depth 2.1 cm corresponding to the distance from the centroid of transverse reinforcement to the bottom surface of the slab.

4.2 Fatigue characteristics

In central pulsating loading, cracks that initially occurred beneath the center spread radially on the bottom surface and later some top surface cracks of a circular arc-form also appeared. The collapse mode was of the punching shear type without fracture of reinforcements. As the mode was quite similar to the static collapse mode, three tests about the same points in the static tests were carried out for each slab.

On the other hand, in repeated moving loadings on a single track, bottom surface cracks independently developed from each loading point and after these cracks crossed each other, the cracking pattern took on a tortoiseshell-like form. Severely cracking occurred only in the earlier stage of loading cycles. Behaviour of the bottom surface cracks was remarkable in that the cracks, parallel to the longitudinal reinforcements, opened considerably when a load situated just above them, but they closed completely when the load was taken away. Thus, by the action of alternate compression and twisting due to repeated movements of the load, the crack faces clapped together and rubbed against each other, so that the crack-widths, remaining with no loading, enlarged. The cracks on the top surface developed from the earlier stage of loading cycles were more numerous than those in the case of pulsating loading at a fixed point, and later on, small pieces of concrete fell due to the breaking of the lower edges of the cracked sections. Near the final stage of the loading cycles, a compressive fracture line resulting from the crushing of the concrete occurred along the transversal center line. Thus, the slabs seemed to collapse in a roof-like mode of yield lines, but they eventually collapsed in a punching shear mode without fracture of the reinforcements. The final cracking pattern and the collapse mode are shown in Fig. 2.

On the other hand, the behaviour under repeated moving loadings on three tracks was similar to that on a single track, but a different point was in that the cracking and the falling of small pieces of concrete rapidly developed just after the loading track was changed.

Table 1 Details of Test Slabs.

Type of Slab	Number of Slab	Sizes, Longl. x Trans. in cm	Depth in cm	Effective Depth in cm	Diameter of Reinforcing Bars in cm	Ratio of Reinforcement, in %	
						Longl.	Trans.
I	10	90 x 260	6	4.5	0.6	1.320	1.320
0	10	90 x 260	6	4.5	0.6	1.320	0.726

The relationship between load level (ratio of the load applied to the average value of static collapse loads) and the total number of loading cycles to failure is shown in Fig. 3. The fatigue life versus load level curves drawn in the figure are determined by the least-squares method, using the data given under identical loading conditions. These load level, R , versus fatigue life, N , curves can be expressed by the following equations:

For isotropic slabs under pulsating loading at a fixed point,

$$R = 1.08 - 0.086 \log N \quad (1)$$

For orthotropic slabs under pulsating loading at a fixed point,

$$R = 1.14 - 0.093 \log N \quad (2)$$

For isotropic slabs under moving loadings on a single track,

$$R = 0.93 - 0.076 \log N \quad (3)$$

For orthotropic slabs under moving loadings on a single track,

$$R = 0.99 - 0.102 \log N \quad (4)$$

If fatigue strengths at 2×10^6 in the total number of loading cycles are predicted from these equations, then the values, 0.54, 0.55, 0.45 and 0.35 are obtained for each case mentioned above.

Obviously, it can be seen that a fatigue life under the same load level is much shorter in the case of moving loadings than in the case of pulsating loading at a fixed point, and the effect of transverse reinforcements on the enhancement of fatigue strength is also greater in the case of moving loadings.

4.3 Stiffness degradation

Relationships between the increase in central deflection (the total amount of elastic and residual deflections) and the total number of cycles are shown in Figs. 4 and 5. Under central pulsating loading, the deflections became rather slow but began to increase rapidly near the time of collapse, and when the deflections reached within a range from 0.25 cm to 0.3 cm, corresponding to about 2.5 times of the theoretical value obtained by an elastic thin plate theory, top surface cracks occurred.

On the other hand, under repeated moving loadings, the deflections gradually progressed from the earlier stage of loading cycles, and when the deflections reached within a range from 0.32 cm to 0.48 cm, top surface cracks occurred; furthermore, when the deflections were within a range from 1.2 cm to 1.6 cm, corresponding to about 1/5 - 1/4 of the depth of the slabs, a compressive fracture line due to crushing of concrete occurred. The deflections just before collapse amounted to 1.7 cm - 2.2 cm under central pulsating loading and 2.1 cm - 3.0 cm under repeated moving loadings, respectively.

4.4 Strains in reinforcements

Variations of strains (excluding residual strains) in reinforcements at the center are indicated in Figs. 6 and 7. In the repetition of the higher load level, the strains of the longitudinal reinforcements happened to exceed to the yield strain at first one round of the movement of load, but there was virtually no subsequent growth. In the repetition of the lower load level, the longitudinal reinforcements did not yield and their strains were almost stable during

Table 2 Test Programs.

Slab	Number of test	Reinforcement	Loading Condition
IS	3	Isotropic	Static
ID	8	Isotropic	Pulsating at a fixed point
IM	5	Isotropic	Repeated Moving on a Single Track
IR	1	Isotropic	Repeated Moving on Three Tracks
OS	3	Orthotropic	Static
OD	6	Orthotropic	Pulsating at a fixed point
OM	5	Orthotropic	Repeated Moving on a Single Track
OR	2	Orthotropic	Repeated Moving on Three Track



all loading cycles. On the other hand, strains of the transverse reinforcements gradually decreased from the initial stage of loading cycles. Such behaviour seems due to the redistribution of stresses resulting from both the internal bond slips of reinforcements and the orthotropy of the flexural rigidity of the slabs. This behaviour was also consistent with the fact that no fracture of reinforcements occurred until the collapses of the slabs.

5. CONSIDERATION ON FATIGUE LIFE UNDER WHEEL LOADINGS

Moving loading used in these tests was performed by transferring, in turn, a loading point to seven discrete points in the transverse direction as shown in Fig. 1. Such a loading procedure was adopted to simulate the continuous movement of wheel loads since bending moment diagrams under loadings at adjacent points sufficiently overlap each other. However, a certain difference in the effect on fatigue failure between such a loading condition and the condition of wheel loading might arise because in the tests, the alternation of loading and unloading was performed at each loading point.

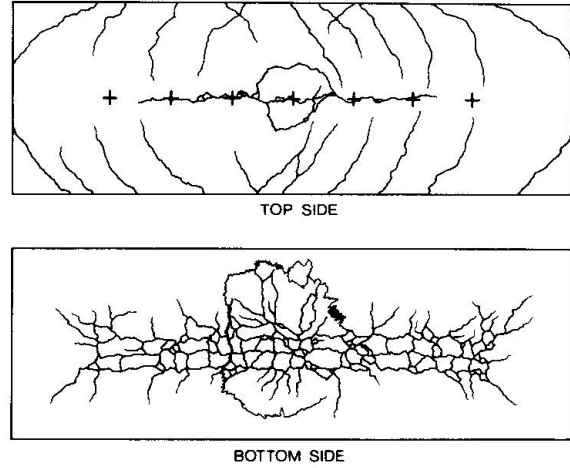


Fig. 2 Final Cracking Pattern in the Slab IM.

Assuming that the partial flexural failure preceding the punching failure controls the fatigue strengths of the slabs, we can examine the contribution of one cycle of loading at each discrete point to the fatigue life of a particular point by using Miner's hypothesis. Denoting the total amount of such contributions by α_j , we obtain,

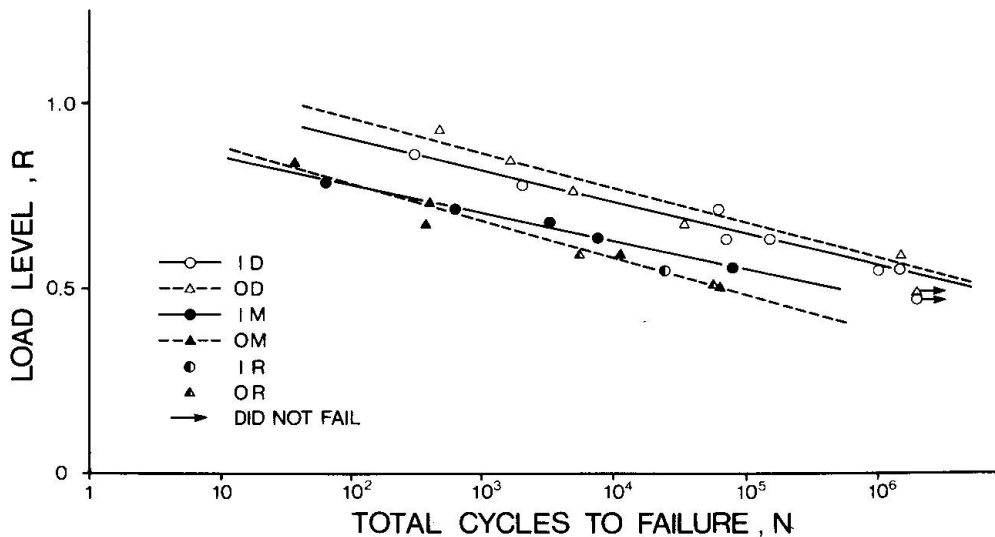


Fig. 3 Relation between Load Level Applied and Total Number of Cycles to Failure.

$$\alpha_j = \sum_{i=1}^r \frac{n_i}{N_{ji}} \quad (5)$$

where, r = number of loading point, N_{ji} = fatigue life of the particular point j under repeated loadings applied at an arbitrary point i , and n_i = cycles of loading applied at the point i . The variation of bending moment at the particular point can be obtained by the elastic thin plate theory,

$$M_j = M_{0j} f(y_j, y_i) \quad (6)$$

where M_{0j} = maximum value of bending moment and $f(y_j, y_i)$ = non-dimensional influence surface whose maximum intensity is reduced to unity, in which y_j and y_i indicate coordinates of the particular point and the loading point, respectively. Using the R-log N curves of Eqs. 1 and 2 for evaluating N_{ji} and using the relation, $R_j = R_0 f(y_j, y_i)$, where R_j = reduced load level to the point j and R_0 = applied load level, the factor, α_j , in Fig. 5 can be expressed as follows:

$$\alpha_j = \sum_{i=1}^r 10^{-M_{0j} [1-f(y_j, y_i)] / \beta K} \quad (7)$$

where $\beta = M_{0j} / R_0$ and K = the gradients of the R-log N curves.

Now, confining our attention on the center of slab and using $r = 7$, $K = 0.09$ obtained from Eqs. 1 and 2 and the influence surface obtained by the elastic thin plate theory, we obtain $\alpha_{j=4} = 1.0002$ and 1.02 for $R_0 = 1.0$ and 0.5 , respectively. Since for any discrete point, being away from the center, a similar result can be expected, it is concluded that the fatigue life of a particular point is scarcely influenced by the loading cycles at other points, and therefore the movement of a load on the seven discrete points aligned becomes equivalent to one passage of a wheel load for an effect on fatigue life.

Thus, from the data in Fig. 3, a comparison of fatigue life under pulsating loading at the center and repeated passages of a wheel load can be given as shown in Fig. 8. It is obvious that the fatigue life becomes much shorter under the condition of wheel-loadings than the condition of central pulsating loadings commonly used in the past studies. If a slab with an isotropic reinforcement fails at 1×10^6 cycles of central loadings, then the slab results in failure at about 1.3×10^4 times of wheel load passage. Further, in an orthotropic reinforcing slab whose transverse reinforcement is reduced to half the amount of the longitudinal reinforcement, a further reduction of fatigue life may be predicted under wheel-loadings.

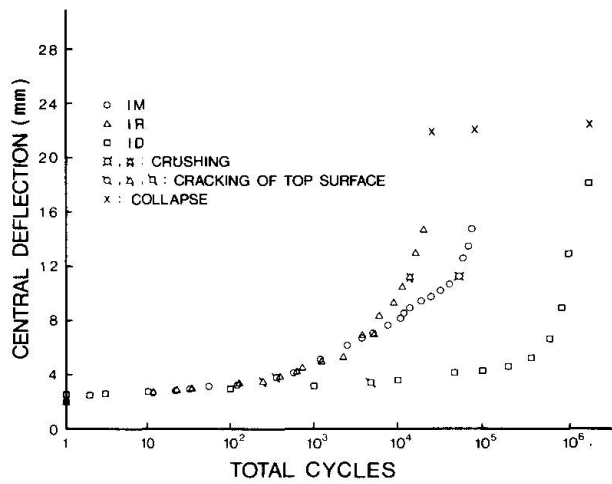


Fig. 4 Growth of Central Deflection under Load 34.3 kN.

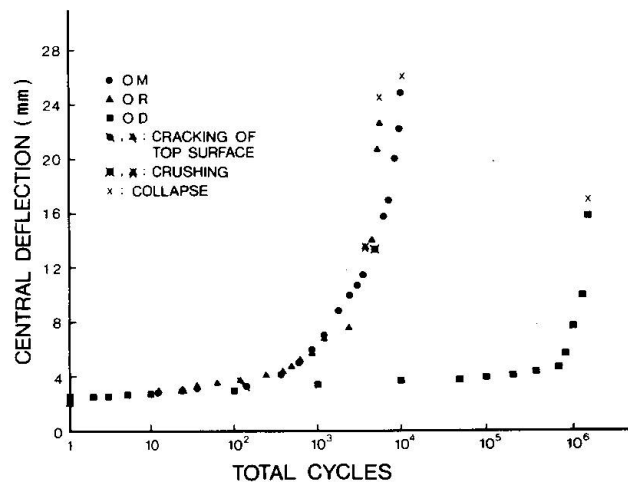


Fig. 5 Growth of Central Deflection under Load 34.3 kN.

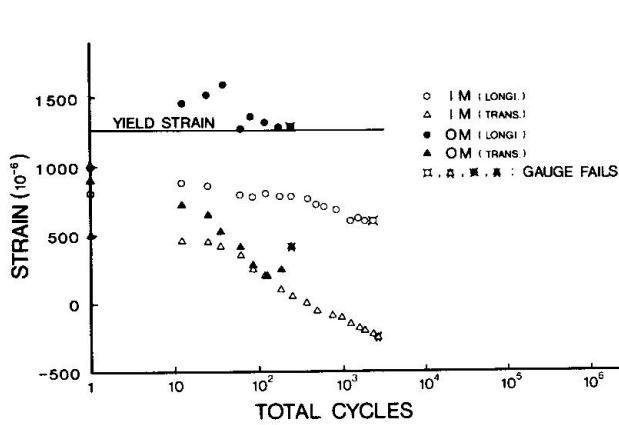


Fig. 6 Strain Variations under Load 39 kN.

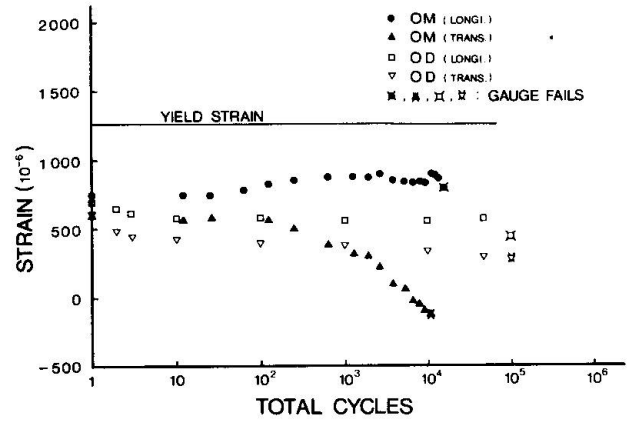


Fig. 7 Strain Variations under Load 29 kN.

6. CONCLUSIONS

The following conclusions can be made:

1. The static load carrying capacities can be predicted with sufficient accuracy by the yield line theory.
2. Damage associated with the development of cracking and the falling of small pieces of concrete occurs from the earlier stage of loading cycles in repeated moving loadings than in pulsating loading at a fixed point.
3. In pulsating loading at a fixed point, fatigue strengths at 2×10^6 cycles amount to more than a half of the static strength, while in repeated moving loadings, the fatigue strengths are predicted to be much lower than this.
4. The effect of transverse reinforcements on the enhancement of fatigue life becomes greater in repeated moving loadings than in pulsating loading at a fixed point.
5. The effect of one passage of a wheel load upon the fatigue failure of slab is equivalent to a range from 80 cycles to 600 cycles of central pulsating loadings.

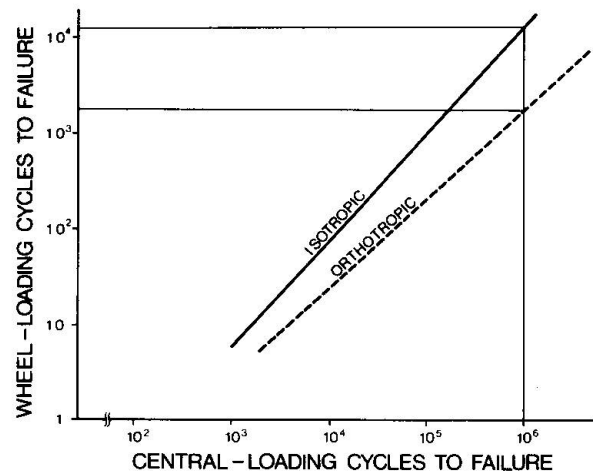


Fig. 8 Relation between Central Loading Cycles and Wheel Loading Cycles to Failure.

REFERENCES

1. Sawko, F. and Saha, G. P.: Effect of Fatigue on Ultimate Load Behaviour of Concrete Bridge Decks, American Concrete Institute Publication SP-26, Concrete Bridge Design, 1971.
2. Hawkins, N. M.: Fatigue Strength of Concrete Slabs Reinforced with Wire Fabric, American Concrete Institute Publication SP-41, Fatigue of Concrete, 1974.
3. Batchelor, B. dev. and Hewitt, B. E.: Are Composite Bridge Slabs Too Conservatively Designed? - Fatigue Studies, American Concrete Institute Publication SP-41, Fatigue of Concrete, 1974.